TECHNICAL REPORT

IEC TR 61282-2

First edition
2003-03

Fibre optic communication system design guides –

Part 2: Multimode and single-mode Gbit/s applications – Gigabit ethernet model

Guides de conception des systèmes de communication à fibres optiques –

Partie 2: Applications Gbit/s multimodales et unimodales – Modèle Gigabit Ethernet

Reference number
IEC/TR 61282-2:2003(E)

Publication numbering

As from 1 January 1997 all IEC publications are issued with a designation in the 60000 series. For example, IEC 34-1 is now referred to as IEC 60034-1.

Consolidated editions

The IEC is now publishing consolidated versions of its publications. For example, edition numbers 1.0, 1.1 and 1.2 refer, respectively, to the base publication, the base publication incorporating amendment 1 and the base publication incorporating amendments 1 and 2.

Further information on IEC publications

The technical content of IEC publications is kept under constant review by the IEC, thus ensuring that the content reflects current technology. Information relating to this publication, including its validity, is available in the IEC Catalogue of publications (see below) in addition to new editions, amendments and corrigenda. Information on the subjects under consideration and work in progress undertaken by the technical committee which has prepared this publication, as well as the list of publications issued, is also available from the following:

- **IEC Web Site (www.iec.ch)**

- **Catalogue of IEC publications**

  The on-line catalogue on the IEC web site (http://www.iec.ch/searchpub/cur_fut.htm) enables you to search by a variety of criteria including text searches, technical committees and date of publication. On-line information is also available on recently issued publications, withdrawn and replaced publications, as well as corrigenda.

- **IEC Just Published**

  This summary of recently issued publications (http://www.iec.ch/online_news/justpub/jp_entry.htm) is also available by email. Please contact the Customer Service Centre (see below) for further information.

- **Customer Service Centre**

  If you have any questions regarding this publication or need further assistance, please contact the Customer Service Centre:

  Email: custserv@iec.ch
  Tel: +41 22 919 02 11
  Fax: +41 22 919 03 00

TECHNICAL REPORT

IEC TR 61282-2

First edition
2003-03

Fibre optic communication system design guides –

Part 2: Multimode and single-mode Gbit/s applications – Gigabit ethernet model

Guides de conception des systèmes de communication à fibres optiques –

Partie 2: Applications Gbit/s multimodales et unimodales – Modèle Gigabit Ethernet

International Electrotechnical Commission, 3, rue de Varembé, PO Box 131, CH-1211 Geneva 20, Switzerland
Telephone: +41 22 919 02 11 Telefax: +41 22 919 03 00 E-mail: inmail@iec.ch Web: www.iec.ch

Commission Electrotechnique Internationale
International Electrotechnical Commission
Международная Электротехническая Комиссия

PRICE CODE U

For price, see current catalogue

CONTENTS

INTERNATIONAL ELECTROTECHNICAL COMMISSION

FIBRE OPTIC COMMUNICATION SYSTEM DESIGN GUIDES –

Part 2: Multimode and single-mode Gbit/s applications – Gigabit ethernet model

FOREWORD

1) The IEC (International Electrotechnical Commission) is a worldwide organization for standardization comprising all national electrotechnical committees (IEC National Committees). The object of the IEC is to promote international co-operation on all questions concerning standardization in the electrical and electronic fields. To this end and in addition to other activities, the IEC publishes International Standards. Their preparation is entrusted to technical committees; any IEC National Committee interested in the subject dealt with may participate in this preparatory work. International, governmental and non-governmental organizations liaising with the IEC also participate in this preparation. The IEC collaborates closely with the International Organization for Standardization (ISO) in accordance with conditions determined by agreement between the two organizations.
2) The formal decisions or agreements of the IEC on technical matters express, as nearly as possible, an international consensus of opinion on the relevant subjects since each technical committee has representation from all interested National Committees.
3) The documents produced have the form of recommendations for international use and are published in the form of standards, technical specifications, technical reports or guides and they are accepted by the National Committees in that sense.
4) In order to promote international unification, IEC National Committees undertake to apply IEC International Standards transparently to the maximum extent possible in their national and regional standards. Any divergence between the IEC Standard and the corresponding national or regional standard shall be clearly indicated in the latter.
5) The IEC provides no marking procedure to indicate its approval and cannot be rendered responsible for any equipment declared to be in conformity with one of its standards.
6) Attention is drawn to the possibility that some of the elements of this technical report may be the subject of patent rights. The IEC shall not be held responsible for identifying any or all such patent rights.

The main task of IEC technical committees is to prepare International Standards. However, a technical committee may propose the publication of a technical report when it has collected data of a different kind from that which is normally published as an International Standard, for example "state of the art".

IEC 61282-2, which is a technical report, has been prepared by subcommittee 86C: Fibre optic systems and active devices, of IEC technical committee 86: Fibre optics.

The text of this technical report is based on the following documents:

Enquiry draft	Report on voting
86C/448/DTR	86C/520/RVC

Full information on the voting for the approval of this technical report can be found in the report on voting indicated in the above table.

This publication has been drafted in accordance with the ISO/IEC Directives, Part 2.

The committee has decided that the contents of this publication will remain unchanged until 2008. At this date, the publication will be

- reconfirmed;
- withdrawn;
- replaced by a revised edition, or
- amended.

INTRODUCTION

The enterprise networking environment has changed significantly in recent years and the available bandwidth to the desktop has greatly increased. This is due to the shift to switch-based networks from hub-based networks that allow the desktop to have full-duplex access to the available link bandwidth. Added to this is the relatively recent increase in the available link bandwidth to the desktop from 10 Mb/s to 100 Mb/s.

One of the drivers for the growth in enterprise bandwidth is the increased use of applications that send large amounts of data over private intranets and the internet. Network traffic is no longer limited to just messages or file transfers; now data streams, such as audio and video, are becoming common, as well as messages with large embedded files. The growth of corporate intranets and the internet has also made network traffic patterns very unpredictable; large files can be accessed from distant places. Within private intranets, there is a growing trend towards using centralized servers. By their very nature, these servers need very high bandwidth connectivity in order to operate effectively.

Due to all these drivers, there is need to increase the bandwidth of enterprise backbone links so that the networks can support the increased demands of the users and prevent congestion. Due to this demand, IEEE 802.3 (ethernet) have developed the next generation standard in the ethernet hierarchy - gigabit ethernet. In the development of gigabit ethernet, it was considered vital that the standard continue to support the installed media base so that network managers can preserve their installation investments. The building backbone links in many Intranets are typically based on optical fibre. The majority of these links are multimode fibre (MMF), however some singlemode fibre (SMF) is also present. Of the current installed base, the dominant type of MMF has a core diameter of 62,5 µm and can have link lengths up to 500 m (550 m including jumper cables).

Gigabit ethernet utilizes an 8B10B code that adds a 25 % overhead to the bit rate resulting in a baud rate of 1,25 Gb/s. The finite modal bandwidth of multimode fibre, particularly 62 MMF at short wavelength, makes meeting the desired bandwidth distance product for gigabit ethernet a serious technical challenge. Added to this, Gb/s rates preclude the use of LEDs due to their slow response times. While lasers have faster response times, their coherence results in additional impairments to link performance such as modal noise and mode partition noise (MPN).

A model was developed as a tool to assist the physical layer committee of the gigabit ethernet (IEEE 802.3z) standard to understand potential trade-offs between the various link penalties associated with laser-based backbone links. An objective for the model was for it to be uncomplicated and able to be implemented in a simple form so that many users could work with it. Another objective of the model is to be applicable to both multimode fibre and single-mode fibre links. The purpose of this technical report is to document the model as used by gigabit ethernet and to identify how it was used to develop the standard specifications.

This technical report presents the theoretical model. Experimental verification is also presented for links operating at valid gigabit ethernet wavelengths of 780 nm, 850 nm and 1 300 nm.

The model is an extension of previously reported models for LED based links [1,2][1]. Power penalties are calculated to account for the effects of intersymbol interference (ISI), mode partition noise (MPN), extinction ratio (ER) and relative intensity noise (RIN). In addition, a power penalty allocation is made for modal noise and the power losses due to fibre attenuation, connectors and splices are included. The model is applicable to single-mode and multimode fibre-based links that incorporate multimode, Fabry Perot or vertical cavity surface emitting laser (VCSEL) lasers. Operation at wavelengths in the 1 300 nm transmission window on multimode fibre includes effects of fibre attenuation, ISI (due to the chromatic and the modal bandwidth of the fibre) and MPN.

Such operation is a more stringent test of the model when compared to operation at wavelengths near 1 310 nm on singlemode fibre. This is because, for the single mode case, fibre attenuation and MPN are the limiting terms. Experimental results for MPN limited operation near wavelengths of 1 310 nm on singlemode fibre can be found in scientific literature [6]. Therefore, this report only includes experimental verification of the model for operation on multimode fibre. In addition, it should be noted that as part of the development of the gigabit ethernet standard, interoperation of single mode fibre links to at least 5 km using transceivers compliant to the IEEE 802.3z specification was demonstrated in agreement with the predictions of the link model.

However, the model described in this report has several limitations as follows.

a) The model ignores chirp. Therefore it should *not* be used to predict dispersion penalties of links incorporating singlemode fibre and directly modulated single frequency lasers since such links are often chirp limited.

b) Optical amplifiers and nonlinear effects, especially significant for dense-WDM (DWDM) systems, and polarization-mode dispersion (PMD), both important for long cable lengths between regenerators, are not treated.

c) Interferometric and reflection-induced power penalties are not included.

d) The model assumes the link components have been designed such that baseline wander is negligible.

e) The model simply adds power penalties or losses in dB. However, for the noise-like terms (MN, MPN, RIN) the variances should have been added and an overall power penalty calculated. However, the error introduced can be shown to be small and within measurement error.

f) For operation on multimode fibre, if single frequency lasers and a non-restricted launch into the fibre are used, the modal noise power penalty allocation may not be correct.

As such the model is intended for non-optically amplified, single-channel systems using multimode lasers (Fabry Perot or VCSEL) and may be used for bit rates up to 10 Gb/s.

---

[1] Numbers in brackets refer to the Bibliography.

FIBRE OPTIC COMMUNICATION SYSTEM DESIGN GUIDES –

Part 2: Multimode and single-mode Gbit/s applications – Gigabit ethernet model

1 Scope

This part of IEC 61282 describes a model developed as a tool to assist the physical layer committee of the gigabit ethernet (IEEE 802.3z) standard to understand potential trade-offs between the various link penalties associated with laser-based backbone links. The purpose of this technical report is to document the model as used by gigabit ethernet and to identify how it was used to develop the standard specifications.

This technical report presents the theoretical model. Experimental verification is also presented for links operating at valid gigabit ethernet wavelengths of 780 nm, 850 nm and 1 300 nm.

The technical report is organized as follows. In Clause 2, a simple theoretical prediction of laser-driven links is presented. Clause 3 contains the description of the experimental measurements and the experimental verification of the theoretical predictions. Finally, Clause 4 contains some example calculations and discussion of the results and use of the model.

2 Theoretical model

The link model is based on a power budget calculation. Power penalties, sometimes referred to as ac penalties, are allocated for link impairments such as noise and dispersion. Power loss is also included to account for connectors and fibre attenuation. The power penalties and losses are added linearly in decibels to determine the total link penalty as a function of length.

In the model, it is assumed that the laser and multimode fibre impulse responses are Gaussian [2]. However, it is assumed that the optical receiver is non-equalized and has a raised cosine response. Additionally, the case where the receiver has an exponential impulse response is stated [2]. The gigabit ethernet standard uses bandwidth and rise time specifications rather than RMS pulse width. Therefore, the model includes expressions that convert the RMS impulse width of the laser, fibre and optical receiver to rise times fall times and bandwidths. These calculated rise times, fall times and bandwidths are used to determine the fibre and composite channel exit response and the ISI penalty of the optical communications link. It is assumed that rise times and fall times are equal and only the rise time is referred to throughout the rest of this technical report. For real components, the larger of the experimentally measured rise or fall time should be used as the input parameter. Rise time refers to the 10 % to 90 % rise time. This can be converted to a 20 % to 80 % rise time by dividing by 1,518 (assuming Gaussian response). In this technical report, equations for penalties or losses are in linear units unless otherwise stated.

2.1 RMS pulse width, rise time and bandwidth

It has been shown [3] that if $h_1(t)$ and $h_2(t)$ are positive pulses and if

$h_3(t) = h_1(t) \otimes h_2(t)$ ($\otimes$ represents the convolution operation) then:

$$\sigma_3 = \sqrt{\sigma_1^2 + \sigma_2^2} \tag{1}$$

where σ_i is the RMS pulse width of the individual components. The 10 % to 90 % rise time, T_i, and bandwidth of individual components, BW_i, are related by constant conversion factors, a_i and b_i, so that:

$$\sigma_i(BW) = \frac{a_i}{BW_i} \tag{2}$$

and

$$\sigma_i(T) = \frac{T_i}{b_i} \tag{3}$$

therefore

$$T_i = \frac{a_i \cdot b_i}{BW_i} \tag{4}$$

Equation (1) can be generalized for an arbitrary number of components:

$$\sigma_s^2 = \sum_i \sigma_i^2 \tag{5}$$

The RMS pulse widths of the individual components may therefore be used to calculate the bandwidth or the 10 % to 90 % rise time of the composite system if the appropriate conversion factors for each individual component are known [2]. For example the overall system rise time, T_{sys}, may be calculated using:

$$T_{sys}^2 = \sum_i \left(\frac{b_s}{b_i} \cdot T_i \right)^2 = \sum_i \left(\frac{a_i \cdot b_s}{BW_i} \right)^2 = \sum_i \left(\frac{C_i}{BW_i} \right)^2 \tag{6}$$

The central limit theorem has been used to show that the composite impulse response of a multimode fibre optic link tends to a Gaussian impulse [2].

For systems or components having a Gaussian impulse response the conversion factors a and b are equal to 0,187 and 2,563 respectively so that C = 0,48 [2]. Hence the relationships between the RMS impulse width (σ), rise time (t_r) and bandwidth are:

$$t_r = 2{,}563 \cdot \sigma \tag{7}$$

and

$$BW_{6dB} = \frac{0{,}187}{\sigma} \tag{8}$$

where BW_{6dB} is the 6 dB electrical bandwidth (3dB optical bandwidth) and:

$$t_r = \left(\frac{0{,}187 \cdot 2{,}563}{BW_{6dB}} \right) = \frac{0{,}48}{BW_{6dB}} \quad (9)$$

The determination of the conversion factor for the receiver is based on the type of receiver used. The optical receiver is assumed to consist of a diode detector followed by amplification stages and a low pass filter to shape the pulse to minimize intersymbol interference and to eliminate out-of-band noise. This type of receiver can be modeled as a raised cosine impulse response [2].

The impulse response has an RMS width of σ_r. If the receiver is excited by a step function then the 10 % to 90 % rise time of the source is [2]:

$$t_r = 2{,}732 \cdot \sigma_r \quad (10)$$

and the electrical 3 dB bandwidth is [2]:

$$BW_{r(3\,dB)} = \frac{0{,}1292}{\sigma_r} \quad (11)$$

Therefore, the conversion factor for the raised cosine receiver, assuming the central limit theorem for the system, is (equation 6):

$$C = a \cdot b_s = 0{,}1292 \cdot 2{,}563 = 0{,}33 \quad (12)$$

The simplest form of receiver is a non-equalized receiver with a single pole filter. This receiver can be modeled by an exponential impulse response and it can be shown that a = 0,1588 and b_s= 2,563 which gives C = 0,407 [2] for this type of receiver.

It was decided by the gigabit ethernet committee that for the gigabit ethernet model a conversion factor of C = 0,35 would be used for the receiver to account for the non-ideal nature of the receiver.

2.2 Dispersion penalties

To calculate the ISI penalty, P_{isi}, the exit response time of the composite channel needs to be calculated. With the assumption that the fibre exit impulse response is Gaussian, equation (6) can be used to calculate the fibre 10 % to 90 % exit response time (T_e):

$$T_e = \sqrt{\left(\frac{0{,}48}{BW_m} \right)^2 + \left(\frac{0{,}48}{BW_{cd}} \right)^2 + T_s^2} \quad (13)$$

where T_s is the 10 % to 90 % laser rise time and BW_m and BW_{cd} are the 6 dB electrical bandwidths due to modal and chromatic dispersion respectively. It is assumed that the fibre has a Gaussian response (C = 0,48). In a singlemode fibre link, the modal bandwidth is infinite.

The approximate 10 % to 90 % composite channel exit response time (T_c) is then:

$$T_c = \sqrt{\left(\frac{0{,}48}{BW_m} \right)^2 + \left(\frac{0{,}48}{BW_{cd}} \right)^2 + T_s^2 + \left(\frac{0{,}35}{BW_r} \right)^2} \quad (14)$$

P_{isi} for a channel having a Gaussian impulse response is approximated by:

$$P_{isi} = \frac{1}{1 - 1{,}425 \cdot \exp\left[-1{,}28 \cdot \left(\frac{T}{T_c}\right)^2\right]} \tag{15}$$

where T is the bit period. This equation is an approximation of the numerical solution given in [4] and it is useful for spreadsheet implementations of the model. It is accurate to within 0,3 dB of the exact solution for ISI penalties up to 5 dB and to within 1 dB for ISI penalties less than 20 dB. This is illustrated in Figure 1 where the numerical solution of [4] is plotted along with equation 15. The error is also plotted.

The bandwidth due to chromatic dispersion of the multimode fibre link, in MHz, is [1,2]:

$$BW_{cd} = \frac{0{,}187}{L \cdot \sigma_\lambda} \cdot \frac{10^6}{\sqrt{D_1^2 + D_2^2}} \tag{16}$$

where:

$$D_1 = \frac{S_0}{4} \cdot \left(\lambda_c - \frac{\lambda_0^4}{\lambda_c^3}\right) \tag{17}$$

and

$$D_2 = 0{,}7 \cdot S_0 \cdot \sigma_\lambda \tag{18}$$

and λ_0 is the zero dispersion wavelength, in nm, of the fibre, λ_c is the laser centre wavelength, in nm, S_0 is the dispersion slope parameter at λ_0 in $ps/\left(km \cdot nm^2\right)$, L is the fibre length in km and σ_λ is the RMS width of the laser spectrum in nm.

The modal bandwidth, BW_m, is dependent on the fibre type, wavelength and launch characteristics. To analyze a specific link, the BW_m should be measured. To do an analysis based on worst-case overfilled launch (OFL) modal bandwidth, refer to a building wiring standard for values. For example, the TIA standard [5] specifies worst-case OFL bandwidths for multimode fibre, which are given in Table 1. This table is provided only as an example. For a specification, refer to ISO/IEC 11801 [21].

Table 1 – Worst-case OFL bandwidths for multimode fibre [5]

	850 nm	1 300 nm
50 MMF	500 MHz·km	500 MHz·km
62 MMF	160 MHz·km	500 MHz·km

Unlike an LED, laser launches do not replicate an OFL in the MMF. This will be discussed in more detail in Clause 4.

Another power penalty due to dispersion is mode partitioning noise (MPN). In a multimode laser, partitioning of laser power between laser modes does not change the total laser output power and does not cause an additional amplitude noise at the laser output. However, when the laser output field propagates through dispersive fibre, different laser modes travel with different speeds. Consequently, power fluctuations between modes lead to an additional noise, MPN, at the fibre output. The power penalty due to MPN has been shown to be [6]:

$$P_{\text{mpn}} = \frac{1}{\sqrt{1-(Q\cdot\sigma_{\text{mpn}})^2}} \tag{19}$$

where the value of the digital signal to noise ratio, Q, is determined by the maximum acceptable bit error rate (BER) using [6]:

$$BER = \frac{1}{Q\cdot\sqrt{2\pi}}\cdot\exp\left(-\frac{Q^2}{2}\right) \tag{20}$$

and

$$\sigma_{\text{mpn}} = \frac{k}{\sqrt{2}}\cdot\left\{1-\exp\left[-(\pi\cdot B\cdot D\cdot L\cdot\sigma_\lambda)^2\right]\right\} \tag{21}$$

where k is the laser mode partition factor ($0 \le k \le 1$), $B = 1/T$ in ps^{-1}, and $D = \sqrt{D_1^2 + D_2^2}$ is the dispersion in $ps/(km\cdot nm)$.

2.3 Extinction ratio, noise and receiver penalties

An extinction ratio power penalty occurs when a non-zero power level is transmitted for a ''zero''. The power penalty is given by [3]:

$$P_\varepsilon = \frac{1+\varepsilon}{1-\varepsilon} \tag{22}$$

where ε is the laser extinction ratio; the ratio of the optical power on a "zero" divided by the power on a "one".

An additional noise term due to the use of lasers is relative intensity noise (RIN). The noise is due to the fluctuations in the output intensity of the laser and the noise variance, σ_{rin}^2, due to laser RIN is typically calculated using the following equation [7], [8]:

$$\sigma_{\text{rin}}^2 = \alpha\cdot BW_{\text{r(6dB)}}\cdot 10^{\frac{RIN}{10}} \tag{23}$$

where RIN is the laser RIN in dB/Hz and α is a scaling factor that is related to the magnitude of the RIN noise and to the optical power level. It is therefore dependent on a number of factors such as extinction ratio and laser bias points. Typical values of α range from 1 to 4 [7]. Considering that in a bandwidth limited channel, the bandwidth of the channel further reduces the effect of the RIN, it can be argued that the above equation makes the RIN penalty pessimistic. Accordingly, the gigabit ethernet committee adopted the following equation:

$$\sigma_{\text{rin}}^2 = \alpha\cdot\frac{0{,}48}{T_c}\cdot 10^{\frac{RIN}{10}} \tag{24}$$

where $\alpha \approx 0{,}55$ for short wavelength links and $\alpha \approx 0{,}7$ for long wavelength links. T_c is the channel exit response time of the link that accounts in a reduction of the RIN penalty as the channel bandwidth reduces with length. The reduction in α to less than 1 results from the assumption that the shape of the bandwidth-limited channel further limits the noise as compared to an ideal brick-wall filter shape. The differing α's result from the specific link lengths at which the channel shape was calculated. However, it should be remembered that some shaping of the noise spectrum is assumed in the actual measurement of RIN [9]. The RIN noise variance equation (24) used by gigabit ethernet is considered slightly optimistic by the authors.

The RIN induced power penalty is then [8]:

$$P_{\text{rin}} = \frac{1}{\sqrt{1-(Q\cdot\sigma_{\text{rin}})^2}} \tag{25}$$

A comparison of the various noise variance expressions that could be used to calculate the RIN penalty are illustrated in Figure 1 for the case of 850 nm transmission on 62 MMF with a RIN value of –117 dB/Hz.

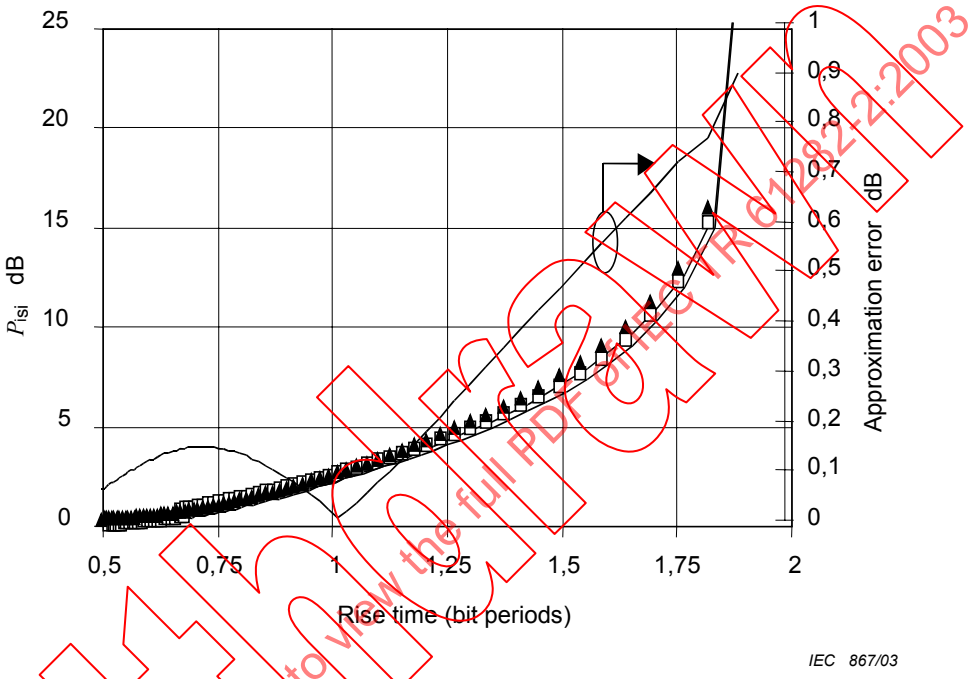

NOTE The maximum error for the approximation is also plotted.

Figure 1 – Comparison of calculated ISI penalty for Gimlett's method [3] (□), and approximation used in this work (▲)

The expression given in equation 23 is plotted for α = 4 and α = 1 as closed triangles and closed squares respectively. The expression used by gigabit ethernet (equation (24)) is plotted as closed diamonds. For comparison, the RIN penalty is calculated considering only the receiver bandwidth and the modal bandwidth as limiting the RIN bandwidth, whereas equation 24 also includes the chromatic bandwidth and the laser rise time. This expression is considered by the authors more realistic and is plotted for the case of α = 4 and α = 1 as open triangles and open squares respectively.

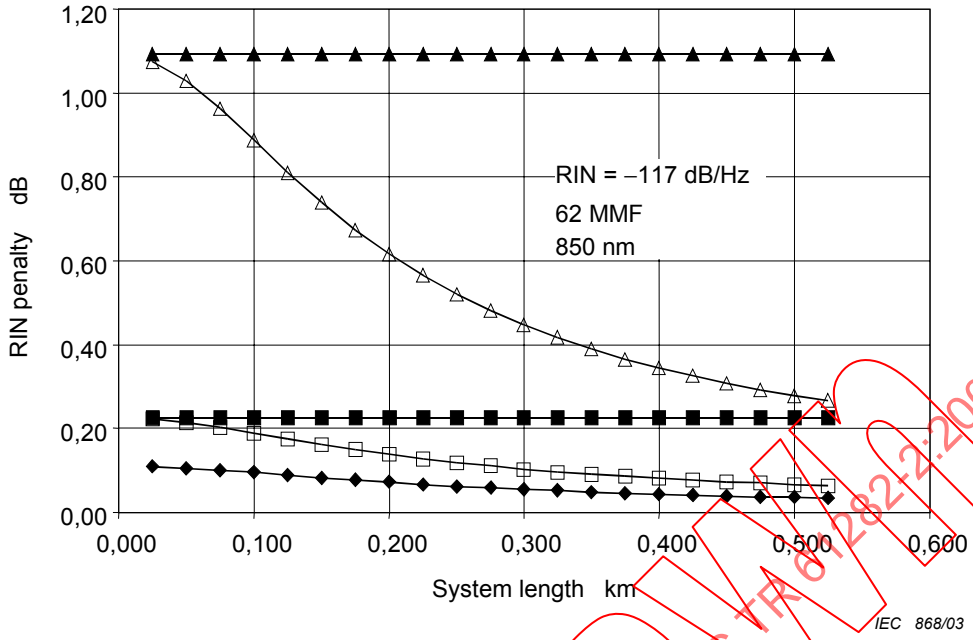

NOTE The RIN penalty plotted here is for Gigabit ethernet equation (24) (◆); Lasky *et al.* equation (23) with α = 4 (▲); equation (23) with α = 1, (■); equation (23) with modal bandwidth included for α = 4 and α = 1 (Δ) and (□), respectively.

Figure 2 – Comparison of RIN penalty versus system length for the different equations

Modal noise is caused by the interference of fibre modes that create a time-varying speckle pattern. When this speckle pattern propagates through a mode selective loss, such as a lossy connector, modal noise occurs. Modal noise penalties depend on the laser characteristics and the link configuration. Consequently, it is difficult to express the penalty as a simple analytical expression. Instead, the theory of [10] can be used to allocate a modal noise penalty.

Finally, a receiver eye opening penalty is included which accounts for the required finite eye opening width needed by the clock and data recovery circuit. The eye opening penalty is calculated as the amount of closure, assuming a raised cosine pulse, at a given width.

$$P_{\text{eye}} = \frac{2 \cdot \sin(\pi \cdot W)}{\pi \cdot W \cdot (1 - W^2)} - 1 \qquad (26)$$

where W is the eye opening width required by the clock and data recovery circuit. W is normalized to the bit period.

2.4 Fibre attenuation

The attenuation, in dB, of cabled optical fibre for a particular length is modeled by:

$$Att = L \cdot \frac{R_\lambda}{C_\lambda} \cdot \left[\left(\frac{1}{9{,}4 \cdot 10^{-4} \cdot \lambda_c} \right)^4 + 1{,}05 \right] \qquad (27)$$

This equation was derived from [11]. The equation is based on the maximum allowable attenuation specifications for MMF, but can be applied to single mode fibre (SMF) in the 1 310 nm region. This equation does not model the OH^- absorption peak at ~1,4 µm. The equation models the shape of the attenuation versus wavelength curve around the two windows of operation and uses R_λ and C_λ as scaling factors. R_λ is the actual cable attenuation in dB/km at either 850 nm or 1 300 nm. For short wavelength links (850 nm) C_λ = 3,5 dB/km and for long wavelength links (1 300 nm) C_λ = 1,5 dB/km. For consistency, the constants within the square brackets have the units that result in a term with units of dB/km.

2.5 Modeling link performance

It is possible to predict the performance of a multimode fibre link, using the equations in this clause. The penalties as a function of link length can all be calculated. To determine the reach of a link, the penalties can be added, linearly in dB, to determine the total penalty as a function of length. If the link budget is known, the maximum link distance is the length at which the total penalty equals the link budget.

An example of this type of calculation will be presented in clause 4 where the link length for some of the gigabit ethernet specifications will be shown.

When using the model it is advisable to keep the accuracy and standard design criteria in mind rather than adhering to the exact number provided by the model. It is possible that the model could predict link lengths that in reality are not feasible due to some large individual penalty contributions. An example of this is the ISI penalty. Blind application of the model will imply that in an ISI limited link, an increase in the link budget will extend the link length. This is true in theory, but in practice, link designers are loath to allow P_{isi} to increase much above certain levels.

Another issue that should be kept in mind is the accuracy of the model. It is estimated that the model is accurate to approximately 10 %. This estimate of the accuracy is due to the combination of the approximations made in the model and the experimental error in the input parameters.

3 Experiment

Two experiments were performed to verify the model. The basic set up is illustrated in Figure 3.

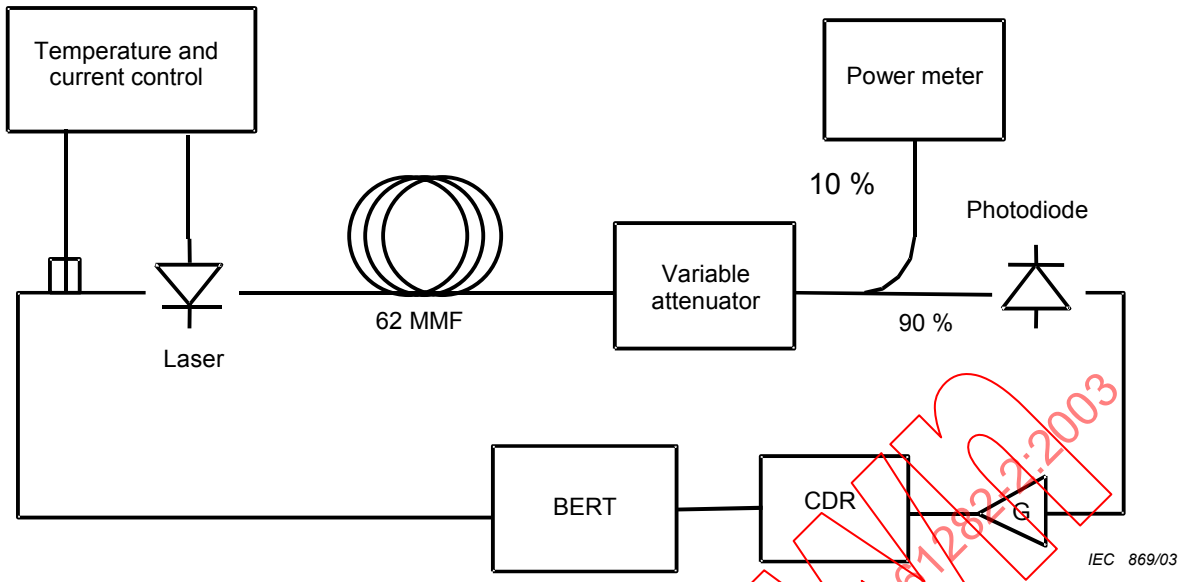

Figure 3 – Experimental set-up for link measurements

A MMF link was built consisting of a laser transmitter, a length of 62 MMF, a variable attenuator, a passive splitter and a photodiode followed by a limiting amplifier and clock and data recovery (CDR) unit.

For these experiments, three laser transmitters of different wavelengths were used: 790 nm, 850 nm and 1 300 nm. The short wavelength lasers were part of transceivers and the 1 300 nm laser was a SC packaged subassembly requiring bias control. All devices were temperature controlled to avoid any temperature fluctuations in order to ensure repeatability.

The penalty of the link was calculated as the difference between the receiver sensitivity at BER $=10^{-9}$ with and without a long length of fibre. The received power was monitored by a power meter attached to the 10 % arm of a 62 MMF coupler. The coupler was of a bulk construction in order to avoid any mode selective losses (MSL). The coupler was measured to have less than 0,3 dB MSL.

The first experiment involved modulating the lasers at the fibre channel rate of 1 062,5 Mb/s and determining the penalty as a function of fibre length. To avoid any effects such as profile equalization, the fibre was chosen to be from the same original spool and was cut into lengths that allowed the link length to be increased by 125 m increments if required. The lasers were modulated with a 2^7-1 PRBS. This PRBS pattern has significantly more DC content and a slightly longer run-length compared to the 8B10B code used by gigabit ethernet.

In the second experiment, rather than varying the link length, the link length was fixed and the bit rate was stepped. This experiment was undertaken in order to remove any effects that connectors might be having on the link performance. The fibre used in this experiment was of one length. Originally it was 2 km long for the measurements at 1 300 nm and it was then cut to 500 m for the measurements at 790 nm and 850 nm. Because the bit rate was varied in this experiment, the CDR was not used and the received data was aligned to the source clock.

Before these experiments were performed, every parameter of the lasers and fibre that would be needed for the model in the experiments was measured. The experimental data was then compared to the theoretical predictions.

3.1 Device characterization

The model requires knowledge of the lasers' rise/fall times, RMS spectral width, RIN and mode partitioning factor, k.

The lasers rise/fall time was measured using a high-speed oscilloscope. The slowest of the 10 % to 90 % rise or fall time was used as the input parameter for the model.

The RMS spectral width was measured using an optical spectrum analyzer. The spectral widths were verified manually with a TIA fibre optic test [12].

The laser RIN was measured as described in [9]. This procedure measures the electrical noise power produced by a photodiode which is connected to a CW laser under test. The electrical noise spectrum is filtered with a 4th order Bessel-Thompson filter at 0,75 times the link bit rate. This method gives a more accurate measure of the laser RIN than measuring the RIN at a spot frequency.

The mode partitioning factor, k, was measured by optically filtering an individual laser mode and then measuring the statistics of its fluctuations on a high-speed oscilloscope [13].

The mode partition factor of each individual mode, k_i, is defined as:

$$k_i = \frac{\sigma_i}{\sqrt{\mu_i - \mu_i^2}} \tag{28}$$

where σ_i is the individual mode's normalized standard deviation and μ_i is the individual mode's normalized mean.

The k of the laser is calculated to be:

$$k^2 = \sum_{i=1}^{N} k_i^2 \quad \text{for N laser modes} \tag{29}$$

The k factor was measured while the laser was being modulated. Due to the pattern dependence of k, it was measured at a number of positions in a repeating pattern. Three positions were chosen: an isolated ''one'', a long string of five ''ones'' and one bit interval within the string of five ones after the laser ringing had damped. The results from these three positions were then averaged to reach a composite k value. An example of the measured traces is illustrated in Figure 4.

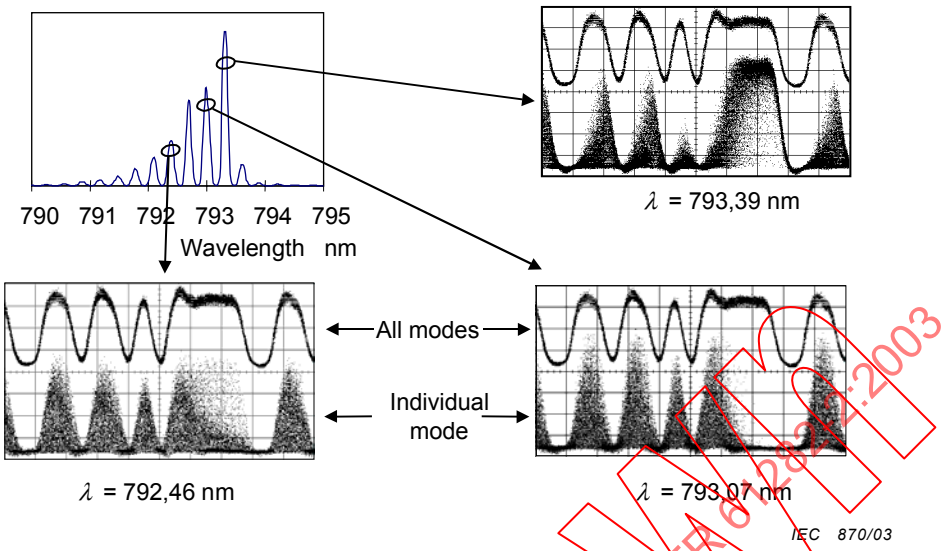

Each oscilloscope trace shows the dynamics of the individual mode (below) and all modes (above). The oscilloscope was used in infinite persistence mode so that the density of the dots is proportional to the probability of occurrence.

Figure 4 – Illustration of mode partitioning behavior in 794 nm Fabry-Perot laser

Figure 4 shows the spectrum of a modulated 790 nm Fabry-Perot laser. Individual modes were filtered using an optical filter with a 0,2 nm passband. The output of the filter was connected to a high speed APD and viewed on the oscilloscope. Figure 4 shows three traces corresponding to the time response of three separate modes. On each scope trace the time response of all the modes together (filter BW of 5 nm) is shown. It can be seen how each mode has distinct behavior. All lasers tested exhibited mode partitioning, but it was observed that not all lasers partitioned in the same manner. There were two typical regimes. The first regime occurred when very few modes had all the power at one instance and the other modes competed for the gain. This behavior resulted in a high k measurement. The laser demonstrated in Figure 4 is an example of a laser partitioning in this manner. The second partitioning regime occurred when all the modes were fluctuating but many modes were present simultaneously. This behavior resulted in a low k measurement.

The modal bandwidth of the fibre was measured using a frequency domain technique. The modal bandwidth of a fibre can be very launch dependent when using an underfilled launch. All lasers underfill the multimode fibre due to their restricted numerical aperture and spot sizes. Therefore, in order to compare the theoretical calculations with the experimental measurements, the fibre's modal bandwidth was measured using the same laser that was to be used in the link measurements. This was referred to as the fibre's effective modal bandwidth (EMB). It was noted that in all cases the EMB frequency responses of the fibres had a Gaussian-like shape. This is not always the case with laser launches and will be discussed later. When the laser could be linearly modulated, the bandwidth was measured using a swept frequency technique [14]. For lasers that were part of transceivers, a digital modulation technique was used to measure the modal bandwidth. This required measuring the difference between the received electrical spectrum and a calibrated electrical spectrum that was measured when a patchcord was used instead of the fibre under test while the laser was modulated with a pseudo-random sequence.

The chromatic dispersion was measured for each fibre by using the technique described in [18]. The delay over a long length of fibre was measured at a number of wavelengths and a curve fitting routine was used to determine the dispersion zero and the dispersion slope parameter. As described in [19], the measurement of chromatic dispersion requires an overfilled launch. In [19] a correction factor is developed for determining the chromatic dispersion of a multimode fibre when a single-mode launch is used. In our experiments, the actual laser sources used for the system measurements were used to measure the delays. Obviously, these sources produced neither overfilled launches nor single-mode launches but since they were lasers, the launches were likely underfilled. It was decided to use the values as measured to determine an 'effective' chromatic dispersion, as it was not clear how to apply the correction factor of [19]. It was found that if the correction factor was used, it did not alter the results noticeably and so it was neglected for the comparison with theory.

The measured laser and fibre parameters are given in tables 2, 3 and 4 respectively.

Table 2 – Measured source parameters

Source #	1	2	3
Type	FP	FP	FP
λ_c (nm)	1 318	857	794
RMS spectral width (nm)	1,5	0,85	0,8
Mode partitioning factor, k	0,5	0,85	0,85
10 % to 90 % rise time (ps)	350	300	300
RIN (dB/Hz)	–137	–125	–120

Table 3 – Fibre parameters for experiment No. 1 (constant bit rate)

	λ_c = 1 318 nm (source No. 1)	λ_c = 857 nm (source No. 2)	λ_c = 794 nm (source No. 3)
EMB (MHz·km)	2000	775	525
Attenuation (dB/km)	0,62	2,98	3,83
Zero dispersion wavelength (nm)	1 377		
Dispersion slope (ps/nm^{2}km)	0,084		

Table 4 – Fibre parameters for experiment No. 2 (constant fibre length)

	λ_c = 1 318 nm (source No. 1)	λ_c = 857 nm (source No. 2)	λ_c = 794 nm (source No. 3)
EMB (MHz·km)	700	234,5	166
Attenuation (dB/km)	0,52	2,71	3,38
Zero dispersion wavelength (nm)	1 398		
Dispersion slope (ps/nm^{2}km)	0,073		
Length (km)	2	0,5	0,5

3.2 Link measurements

The first experiment measured the link penalty as a function of link length. The links were operated at the fibre channel rate of 1,062 Gb/s. Using the parameters listed in Tables 2 and 3, the theoretical performance was calculated. The comparisons are illustrated in Figures 5, 6 and 7 for the links operating at 1 318 nm, 857 nm and 794 nm respectively.

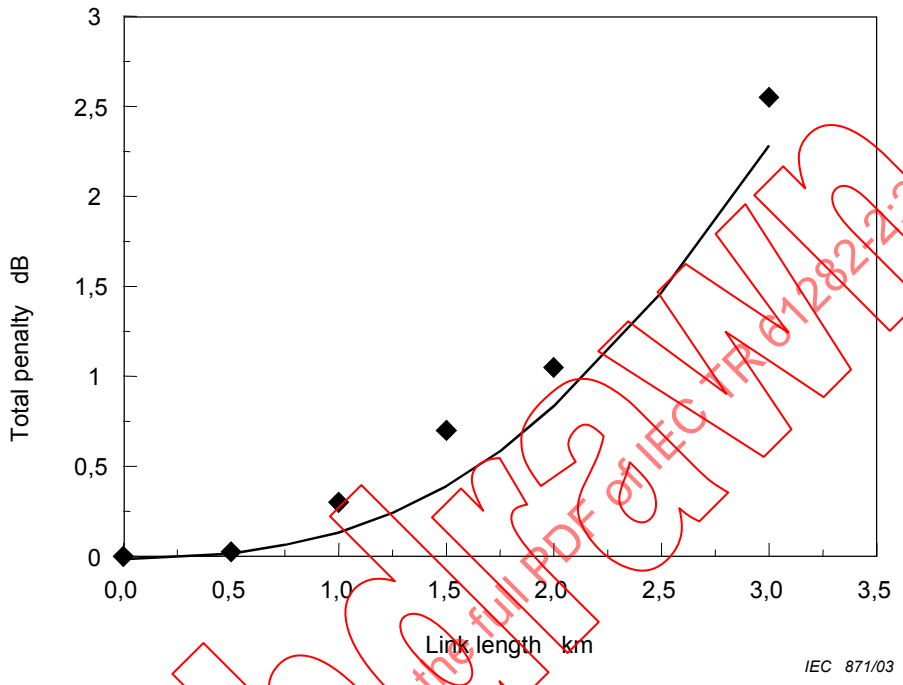

NOTE Theoretical prediction (——) and measured penalty(◆).

Figure 5 – Penalty versus distance for source No.1 (1 318 nm)

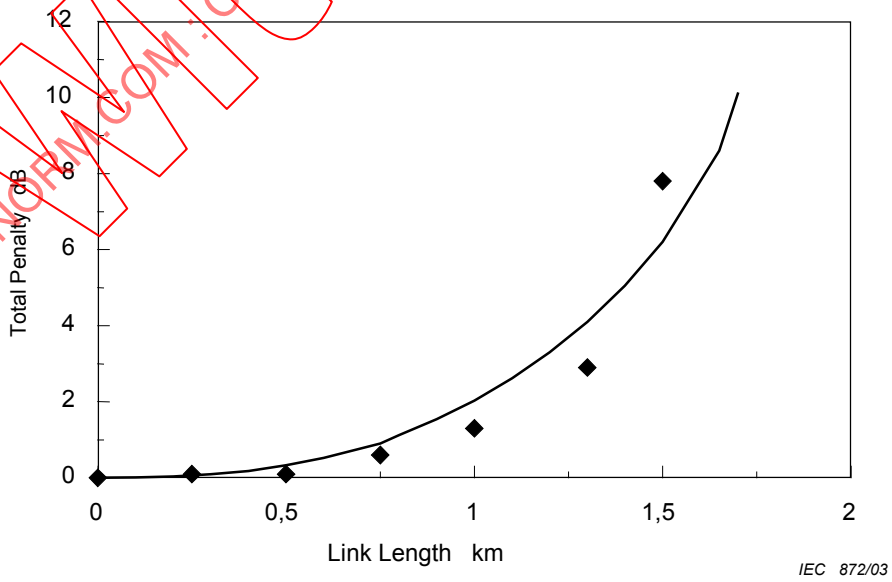

NOTE Theoretical prediction (——) and measured penalty(◆).

Figure 6 – Penalty versus distance for source No. 2 (857 nm)

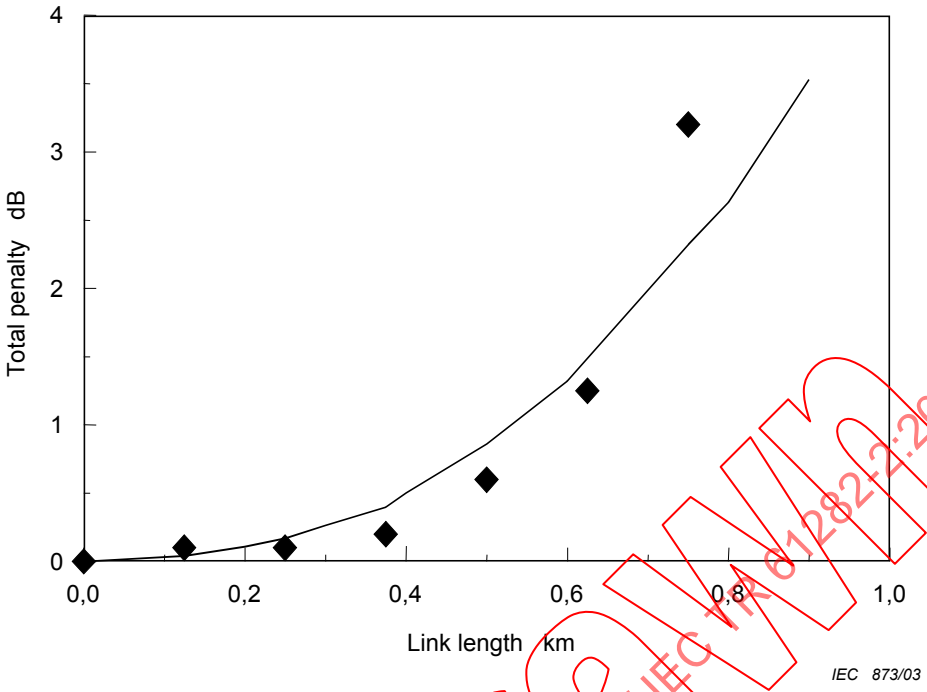

NOTE Theoretical prediction (——) and measured penalty(◆).

Figure 7 – Penalty versus distance for source No. 3 (794 nm)

It can be seen that there is good agreement between the measured link penalty and the theoretically calculated penalty. The agreement between experiment and theory deviates mostly towards the longer link lengths where the ISI penalty is getting large. As stated earlier, the accuracy of the P_{isi} approximation decreases with increased ISI. Another factor exacerbating the problem is the accuracy of the modal bandwidth measurement. The P_{isi} penalty is exponentially dependent on the modal bandwidth. In recent modal bandwidth round robin tests conducted by the TIA FO2.2 group, repeatability of the bandwidth measurement was found to be within 10 % for a single measurement set-up.

Another issue that was difficult to control in this experiment was the effect of the connectors. The links were made up from combinations of 1 000 m, 500 m, 250 m and 125 m lengths of the same original fibre. Each length used in the experiment was built up using the minimum number of pieces but there was still concern about connector effects. The main concern was that due to the connector tolerances, slight mismatches could result in different launch conditions in the fibre and result in slightly different modal bandwidths. Typically this would not be a major problem but for the sake of matching experiment to theory, a second experiment was performed using one length of fibre and varying the bit rate instead.

The results of the second experiment are plotted in Figures 8, 9 and 10 for the links operating at 1 318 nm, 857 nm and 794 nm respectively. Again, there was good agreement between the theory and experiment. In this experiment there was less scatter of the data around the calculated line which was attributed to the lack of connectors in the link.

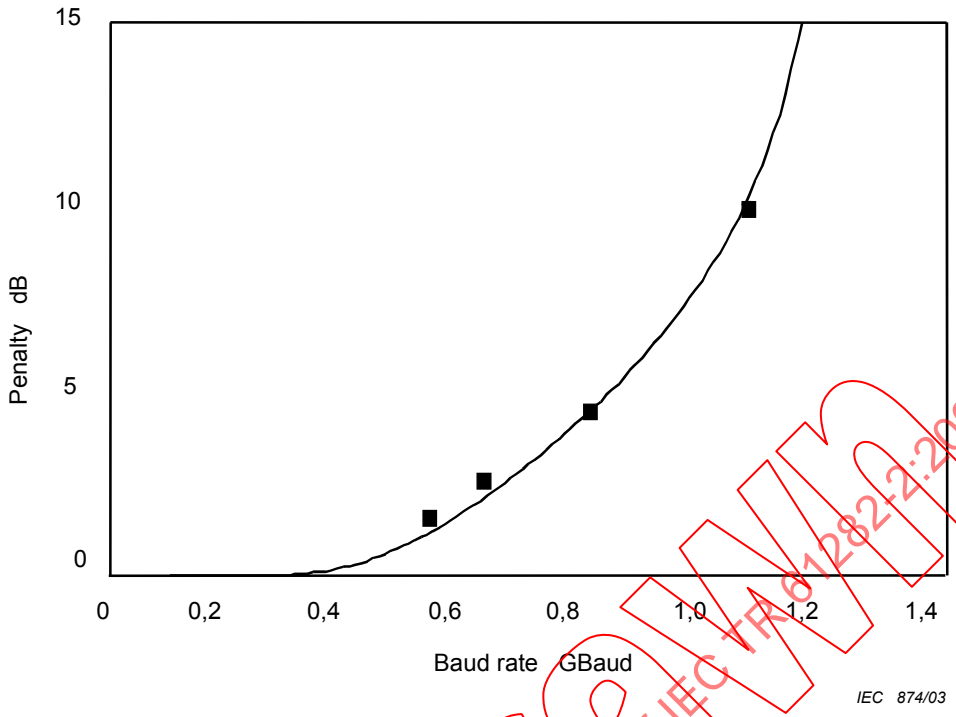

NOTE Fibre length = 2 km. Theoretical prediction (——) and measured penalty (■).

Figure 8 – Penalty versus Baud rate for source No. 1 (1 318nm)

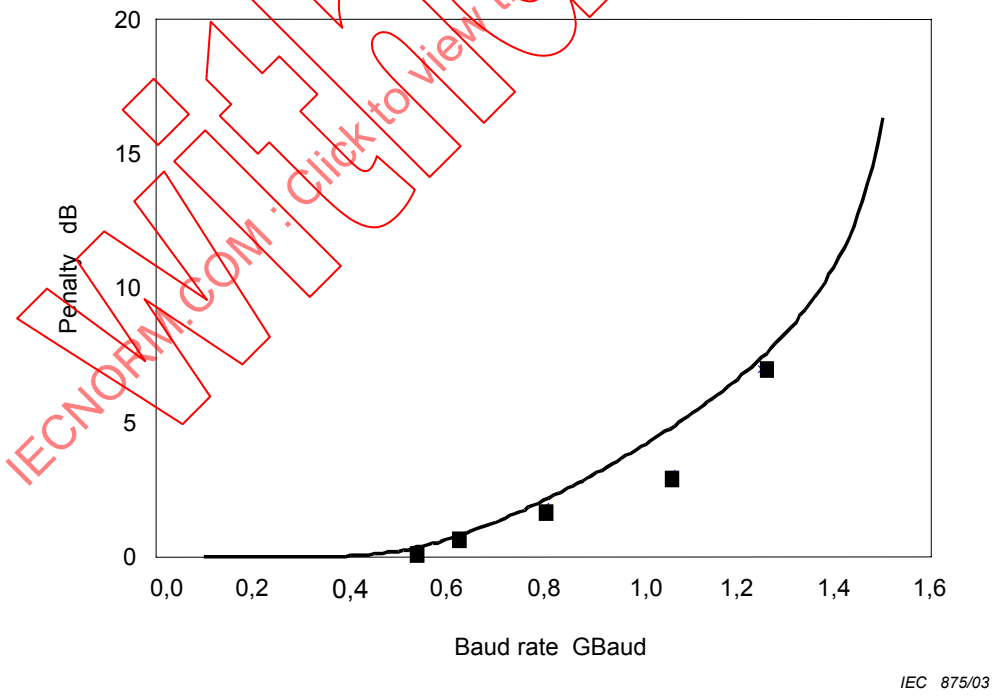

NOTE Fibre length = 0,5 km. Theoretical prediction (——) and measured penalty (■).

Figure 9 – Penalty versus Baud rate for source No. 2 (857nm)

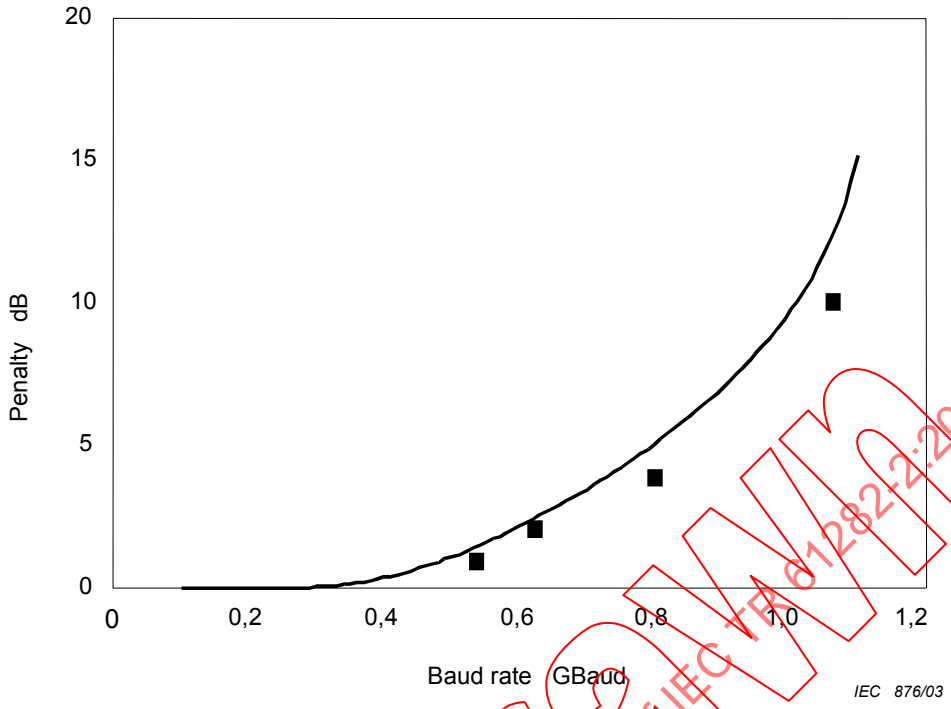

NOTE Fibre length = 0,5 km. Theoretical prediction (——) and measured penalty (■).

Figure 10 – Penalty versus Baud rate for source #3 (794 nm)

Based on these sets of experiments and the independent confirmation from a number of other companies participating in gigabit ethernet, the model was accepted as the working tool of the committee.

4 Examples and discussion

The calculations of the worst-case link lengths for gigabit ethernet operating on 62 MMF are illustrated in Figures 11 and 12 for 850 nm and 1 300 nm operation respectively. The values used in the model are the worst-case specifications defined in the IEEE 802.3z standard [15] and are given in Table 5.

To determine the maximum link distance, the length at which the penalties add up to the maximum allowable value is determined. The maximum allowable penalty is calculated as the power budget minus the fixed passive losses or connector losses as shown in Figures 11 and 12.